Journal of Materials Chemistry

Cite this: *J. Mater. Chem.*, 2011, **21**, 3485

www.rsc.org/materials

PAPER

New role of graphene oxide as active hydrogen donor in the recyclable palladium nanoparticles catalyzed ullmann reaction in environmental friendly ionic liquid/supercritical carbon dioxide system†

Jinsheng Cheng,*[ab] Gencheng Zhang,[a] Jin Du,[b] Longhua Tang,[c] Jingying Xu*[d] and Jinghong Li[c]

Received 24th July 2010, Accepted 4th January 2011
DOI: 10.1039/c0jm02396e

An economical and green pathway: graphene oxide (GO)-supported palladium nanoparticles (Pd NPs) catalyzed a reductive Ullmann reaction of aryl chloride towards biaryl with high conversion and selectivity in ionic liquid (IL)–supercritical carbon dioxide ($ScCO_2$). The combination of IL and $ScCO_2$ provides superior advantages in product separation, catalyst recycling and reuse of the reaction media over traditional organic solvents. Further investigations showed that GO, the novel catalyst support bearing abundant carboxylic, hydroxyl, epoxy and aldehyde groups, can replace the traditional active hydrogen donor readily with much enhanced product separation efficiency. The use of IL, *e.g.* [hmim][Tf_2N], led to obvious improved stability of the Pd NPs, which was helpful for catalyst recycling. Carbon dioxide, a naturally abundant, nonflammable, relatively nontoxic, economical and recyclable "greenhouse" gas, was found to significantly promote the selectivity of the graphene oxide-based Pd NP-catalyzed reductive Ullmann reaction of aryl chloride. Investigations showed that the Pd NP catalyst and IL can be recycled for more than 5 runs without obvious loss of conversion, indicating the economical viability of this process.

Introduction

There are increasing interests in the development of environmentally friendly and economically viable transition-metal catalyzed processes, feasible innovative methodologies including "clean" reaction media applications, catalyst immobilization and recycling, reuse of the reaction media and high efficient product separation, *etc.*[1]

Among various approaches, combinations of IL with supercritical fluids, particularly $ScCO_2$, offer a highly attractive choice. By combing with ILs, the dissolved CO_2 significantly increases the mass transport properties of the IL phase. And typically, ILs can dissolve large amounts of CO_2, but ILs are usually insoluble in $ScCO_2$, thus the IL–$ScCO_2$ system has gained importance in separation and catalysis reactions, in which the catalyst is trapped in the IL phase, and the reactant and product can be added and removed from CO_2 phase.[1c,2a] Furthermore, multiple options can be used to adjust the solvent properties; there are a vast selection of cations and anions to tailor the IL properties, and temperature and pressure can also be varied to regulate the density and solvent power of $ScCO_2$.[2]

Over the past decades, the IL–$ScCO_2$ system has received increasing amounts of attention in separation, chemical reaction and material synthesis.[2a,3] For example, Baiker and co-workers performed Pd–[bmim][PF_6] catalyzed hydrogenations in an IL–CO_2 biphasic system with efficient product separation.[4] The catalytic system exhibited excellent activity and selectivity and showed no obvious deactivation during the reaction cycles. Similarly, Cole-Hamilton and co-workers have developed a continuous flow homogeneous catalytic process for the hydroformylation of long chain alkenes in IL–$ScCO_2$. The catalyst remained in the reactor at all times, CO_2 could also be recycled and no other solvents were required.[5] Wai *et al.* studied the recyclable palladium chloride catalyzed Heck reaction in an IL–$ScCO_2$ biphasic system and found that the coupling efficiency was dependent on the water content of the ionic liquid.[6]

Another important issue for environmentally and economically important organic transformations was a recyclable transition-metal, *e.g.* NPs, which catalyzed reactions with high activities and selectivity. Therefore, designing new catalysts by combining transition-metal NPs with an efficient support of choice instead of complicated ligands provides a broad scope for

[a]*School of chemistry and chemical engineering, Yancheng Teachers University, Yancheng, 224003, China*
[b]*Department of Chemistry, Youjiang Medical University for Nationalities, Baise, 533000, China*
[c]*Department of Chemistry, Tsinghua University, Beijing, 100084, China*
[d]*Tongji Eye Institute and Department of Regenetive Medicine, Tongji University School of Medicine, Shanghai, China*

† Electronic Supplementary Information (ESI) available: Materials and characterization, synthesis procedure for the graphene oxide, supplementary characterization of the recycled catalyst, structures of the ionic liquids together with details of the spectroscopic data of the biaryls **2a–i**. See DOI: 10.1039/c0jm02396e/

the discovery of novel, highly selective and recyclable catalysts for further applications.[7]

Graphene, defined as a two-dimensional honeycomb lattice of carbon atoms, has attracted major attention due to its excellent mechanical, thermal and electronic properties.[8] In recent years, various NP–graphene composites have been fabricated, such as precious metal–graphene,[9a–c] TiO_2–graphene,[9d] CdS–graphene *etc.*,[9e] in which graphene serves as the new catalyst support. These NP–graphene composites show good catalytic performance in organic transformations, direct methanol fuel cells, photocatalysis and photoelectrochemical cells *etc.*

In quite a few reports, GO was primarily used as the precursor of reduced graphene oxide or functionalized graphene nanomaterials, and gained a tremendous amount of excitement owing to its remarkable electronic, mechanical, and chemical properties.[10] While currently, little attention has been paid to GO as an active hydrogen donor.

As one of the most important intermediates, biaryls are key building blocks of numerous biochemicals,[11] pharmaceuticals,[12] agrochemicals, dyes,[13] sensors,[14] conductive polymers[15] and helpful ligands for asymmetric catalysts,[16] *etc.* The original and most widely used methodology to access them was *via* the Ullmann reaction, homocoupling of aryl halides.[17,18] It is usually carried out with copper as the catalyst, however, an excess of copper or harsh reaction conditions[18b,19] were necessary. An effective and milder catalytic alternative was the palladium-catalyzed reductive coupling of aryl halides.[17c–f] In these processes, reducing agents such as aldehydes,[17e] hydrogen gas,[20] alcohols,[21] carbon monoxide,[22] ascorbic acid,[23] amines,[24] zinc[17f] or indium,[13a] *etc.* were required for closing the reductive coupling cycle. Due to the wide applications of the Ullmann reaction, the development of economical, environmental friendly methods was crucial important. Traditional works on Ullmann reaction were mostly performed in volatile organic solvents. In recent years, some researchers focused their interests on the Ullmann reaction in clean reaction media, such as poly(ethylene glycol),[25] $ScCO_2$[26] (or liquid CO_2[27]) and ILs,[17e] *etc.* However, most of the work encountered various difficulties, such as volatile chemical (co-solvent or reductant) employment, waste of reaction media, poor catalyst recycling and inefficient product separation, *etc.* For example, Cotugno and co-workers reported an aldehyde promoted Ullmann reaction of vinyl and heteroaryl halides in tetraalkylammonium ILs under mild conditions.[17e] However, the amount of IL used for only 1 run led to unnecessary waste and environmental pollution, and the application of the toxic aldehyde, which was poorly miscible with the IL, to extract the reaction products diminishes the overall simplification of the recycling and can go as far as causing contamination of the IL.

Therefore, the combination of ILs and $ScCO_2$, which can provide superior advantages in product separation, catalyst recycling and reuse of IL, would be an excellent alternative "green" choice. Unfortunately, until now, few works have demonstrated the Ullmann reaction in an environmentally benign IL–$ScCO_2$ system. Herein, we report the economical attractive reductive Ullmann reaction of aryl chloride over GO-based Pd NPs to biaryls with high conversion and selectivity in an environmentally friendly IL–$ScCO_2$ system, which utilized cheaper aryl chlorides (instead of expensive aryl bromides or aryl iodides) and aluminium (instead of expensive zinc or indium or volatile aldehyde, *etc.*). GO, the novel catalyst support bearing abundant carboxylic, hydroxyl, epoxy and aldehyde groups, can replace the traditional active hydrogen donor (H_2O, *etc.*) readily with much enhanced product separation efficiency. The use of ILs, *e.g.* [hmim][Tf_2N], led to obvious improved stability of the Pd NPs, which was helpful for catalyst recycling. Another reaction media: CO_2, a naturally abundant, relatively nontoxic, economical and recyclable "greenhouse" gas, was found to promote the selectivity of the reaction. Investigations showed that the IL and Pd NPs involved in the IL–$ScCO_2$ system can be used more than 5 times, providing a mild, economic, and green route for the synthesis of symmetric biaryls (Scheme 1).

Experimental

Typical procedure for Pd NP–GO preparation

GO was prepared according to a modified Hummers method.[28] To obtain the Pd NP–GO composites, 10.5 mg GO was dissolved in 48 ml water by ultrasonic treatment for 1 h, and 2 ml 0.02 M $PdCl_2$ was then added under stirring. Successively the pH value of this mixture was adjusted to 10 using 1 M NaOH. Then 240 mg $NaBH_4$ was added slowly to the mixture, the mixture was stirred for 48 h under room temperature. Finally, the solid sample with Pd loading was collected after washing extensively with ethanol and deionized water, removing the unsupported Pd (II) cations completely The sample was then vacuum-dried at 40 °C, giving the catalyst: GO-supported Pd NPs.

Typical procedure for Ullmann reaction in IL–$ScCO_2$

Aryl chloride (2 mM), Al(0) (108 mg), [hmim][Tf_2N] (3 mL) and Pd NPs (3.0% *w*/*w*, 186.2 mg) were added into a 10.0 ml high-pressure stainless vessel, which was sealed and connected to a CO_2 supply. The vessel was charged with CO_2 gradually until a pressure of 5.0 MPa was obtained and heated at 45 °C to a stabilized pressure of 7.0 MPa, then more CO_2 was added to obtain a pressure of 15.5 MPa. The system were stirred under the above conditions for 10 h. Successively, the stirrer and temperature controls were then switched off, CO_2 gradually released

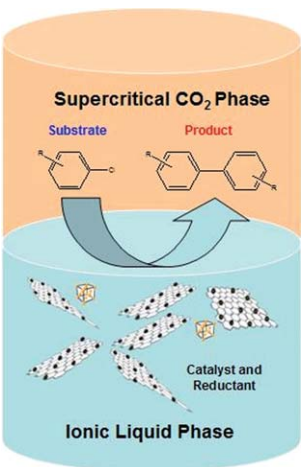

Scheme 1 Illustration of Pd NP–GO catalyzed Ullmann reaction in an IL–$ScCO_2$ system.

into the solvent trap (20.0 ml), while the IL and Pd NPs remained in the reactor vessel for further reaction. The solvent trap vessel was then disconnected and allowed to cool. By simply further decompressing the CO_2, the Ullmann products were collected through the valve on the bottom of the solvent trap conveniently. The resulting organic solid was washed with ethanol and purified with TLC to give the products.

Results and discussion

Catalyst preparation

To synthesize the supported NP catalysts, a yellow-brown dispersion of GO was added to a $PdCl_2$ solution in water The pH value of this mixture was adjusted, $NaBH_4$ was added slowly to the mixture under stirring, then the mixture was stirred at room temperature. Finally, the solid sample with Pd loading was collected after thorough washing with ethanol and deionized water, and vacuum-dried, affording the supported catalyst: Pd NPs/GO (Scheme 2).

The AFM image in Fig. 1 shows that the catalyst support, GO nanosheets with 300–1000 nm lateral width, were mostly single layered (height ~0.9 nm).[29] The supported catalyst, Pd NP–GO was characterized by transmission electron microscopy (TEM), high-resolution transmission electron microscopy (HRTEM), scanning electron microscopy (SEM), electron diffraction (Fig. 2) and XRD spectroscopy (Fig. 3).

Fig. 2a shows the TEM image of Pd NP–GO. It was easy to see that the GO nanosheets were decorated uniformly by the nano-sized Pd particles, which were in the size range 2–10 nm, and few particles were free from the supports, indicating a strong interaction between the particles and GO supports. The above results reveal that the present method can produce stable and small sized Pd NPs. From Fig. 2b, a HRTEM image taken of the surface of Pd NP–GO, we can also observe that the Pd NPs have clear polycrystalline structures, the lattice spacing of which is 0.23 nm, similar to the Pd (111) lattice spacing. The electron diffraction pattern shown in Fig. 2c indicates that the NPs supported on GO have a uniform and narrow particle size distribution, which was also confirmed by the SEM images in Fig. 2d. The polycrystalline nature of Pd NPs produces four X-ray diffraction rings in sequence from inner to outer and can be indexed to the (111),

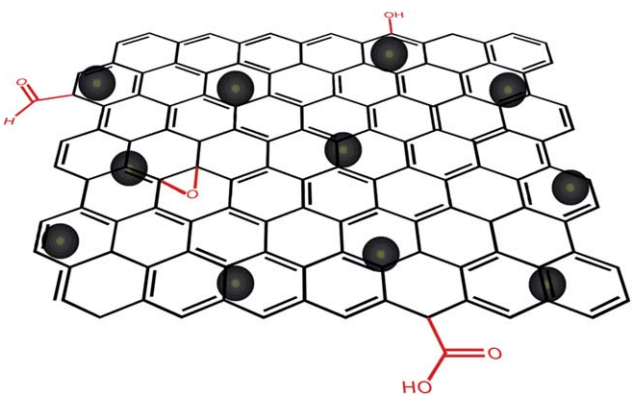

Scheme 2 Illustration of Pd NP–GO, some unreduced carboxylic, hydroxyl and aldehyde groups remained on the GO surface.

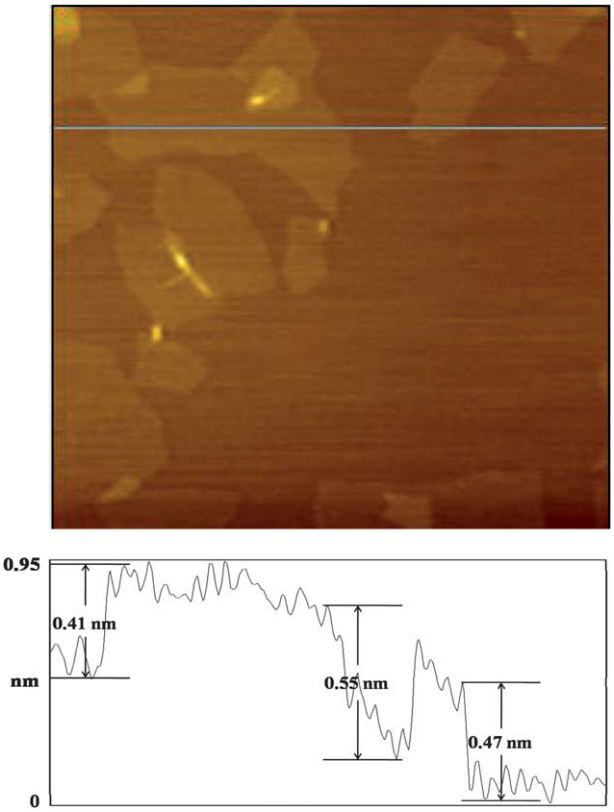

Fig. 1 AFM image and depth profile of GO on mica substrate. Size 2.0 × 2.0 μm.

(200), (220), and (311) of the face-centered cubic Pd planes, respectively. XRD patterns in Fig. 3 show an obvious (002) peak and a strong distinct peak at 11.1° corresponding to a d-spacing of approximately 7.96 Å that is due to interlamellar water trapped between hydrophilic GO sheets, revealing the catalyst is a GO-based composite.[30] The spectra in Fig. 3 also confirmed the maintained presence of crystalline Pd (0) in Pd NPs/GO. The

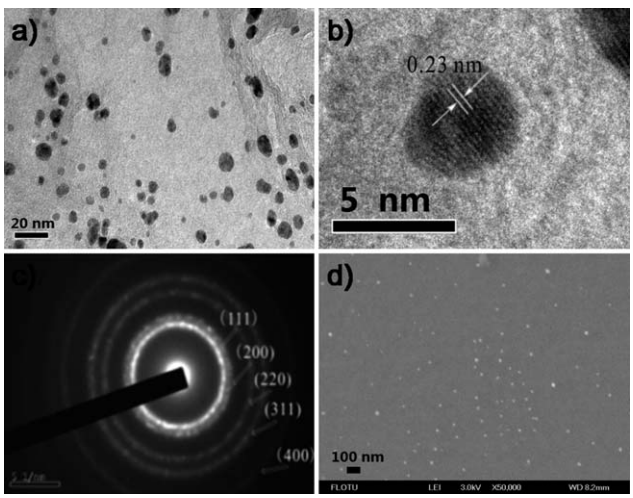

Fig. 2 (a) TEM image of Pd NP–GO; (b) HRTEM image Pd NP–GO, showing the polycrystalline structure of palladium; (c) electron diffraction pattern of Pd NP–GO and (d) SEM image of Pd NP–GO.

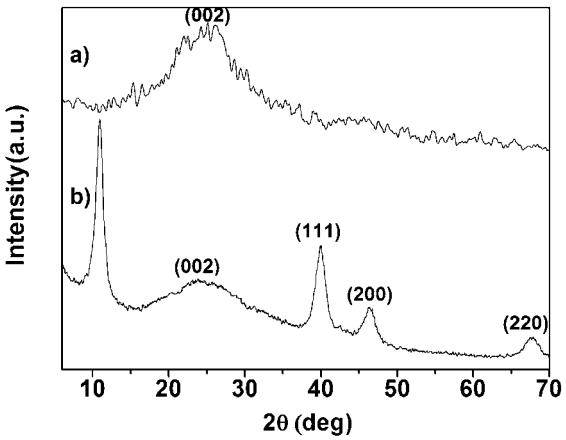

Fig. 3 XRD spectra of graphene (a) and Pd NP–GO (b).

most representative reflections of Pd (0) are indexed as face-centered cubic (fcc) with unit cell parameter $a = 0.390$ nm. The Bragg reflections at 39.6°, 45.5° and 67.3° correspond to the indexed planes Pd (0) (111), (200), (220) of the crystals.

EDS analysis in Fig. 4 reveals that GO bears large amounts of oxygen-containing groups. Similar results were confirmed by FTIR spectra of GO and Pd NP–GO. As we can see from the FTIR spectra the starting material of GO bears large amounts of active hydrogen donor groups (peak at 3200–3400 cm^{-1}, –OH and –COOH groups), thus it could act as novel hydrogen donor. While after 8 catalytic cycles, the peak of Pd NP–GO at 3200–3400 cm^{-1} became much weaker, indicating that the majority of active hydrogen donor groups were consumed in the previous cycles.

The phase behaviour of the IL–$ScCO_2$ system

$ScCO_2$ has been shown as an environmentally benign solvent with tunable physicochemical properties for increasing reactions, and IL can be molecularly engineered for specific physicochemical properties through various "R–" groups and cation/anion selection, *e.g.* viscosity, solubility, density, temperature range, acidity/basicity, co-ordination properties, *etc.* Thus, an IL–CO_2 system draws on the advantages of each of the respective technologies and helps overcome their challenges.[2d] The IL phase in this unique system is employed to sequester the catalyst and the CO_2 phase becomes the mobile phase for reactants and products. Under high pressure, CO_2 can become miscible with IL, thus eliminating gas–liquid phase boundaries and their inherent mass transfer limitation. Furthermore, CO_2 is very soluble in the IL and reaches approximately 40% mol CO_2 at 50 bar, 65% mol at 100 bar, only marginal increase in solubility beyond 100 bar.[2a] In contrast, the IL is immeasurably insoluble in the pure CO_2 phase and does not become miscible (critical) even at hyperbaric pressures, *e.g.* 73.8 bar. More fortunately, the catalyst, *e.g.* GO-based Pd NPs, is far more soluble in IL than it in $ScCO_2$, thus there is no tendency of the $ScCO_2$ to extract the catalyst. One then obtains essentially pure products from the CO_2 flow, contaminated with no IL or catalyst, the catalyst solution left behind in the vessel can be reused for several runs, while the conversion remained high through the cycles.

Scheme 3 shows a schematic of the effect of pressure on the phase behavior of a reaction system that consists of IL, CO_2 and organic (Org.) compounds (reactant and product). When the Pd NP–GO and substrate (Ar–Cl, *etc.*) solution of IL was exposed to CO_2, large amounts of CO_2 dissolved in the IL, causing the liquid solution to expand forming a vapor–liquid equilibrium (VLE). Further addition of CO_2 causes the liquid phase to split into two liquid phases in equilibrium with a vapor phase (vapor–liquid–liquid equilibrium (VLLE)) at the lower-critical endpoint (LCEP) pressure (73.8 bar, step II, Scheme 3). As pressure further increased, the relative volume of the organic-rich phase increases until it reaches the K-point pressure, where the vapor phase and the organic-rich liquid phase merge into a single supercritical phase (SCF). Above the K-point pressure, the SCF phase (organic-rich phase) and the IL rich phase become critical and miscible with each other[31] (some authors also believed that under such conditions, the SCF phase and IL phase can be forced to form one homogeneous liquid phase[32]), thus under such conditions, the reaction can be carried out with much higher activities compared with the heterogeneous system. With the reaction proceeding (step III, Scheme 3), more and more of the

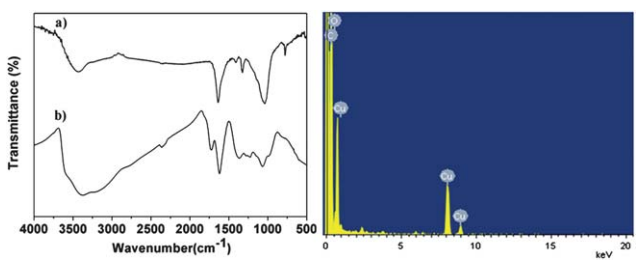

Fig. 4 FTIR spectra (left) of the Pd NP–GO catalyst after 8 cycles (a) and GO (b), energy-dispersive X-ray spectroscopy (EDS) analysis of GO (right).

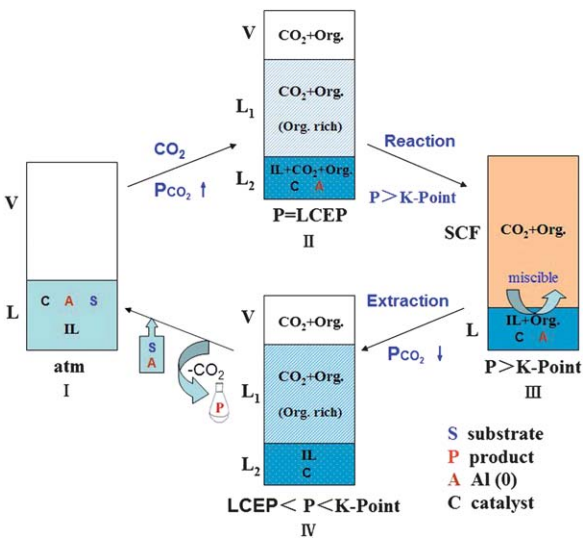

Scheme 3 Schematic views of the "green" pathway of the Ullmann reaction. The catalytic cycle consists of cycle preparation (I), $ScCO_2$ extraction of the substrate (II), SCF phase and IL + Org. phase formation (III) and $ScCO_2$ extraction of the product (IV), after which new substrate and Al (0) can be added to restart the new catalytic cycle.

remaining amount of organic compounds in the IL phase transferred gradually to the upper SCF phase, similar to supercritical fluid extraction from ILs. For the case of complete conversion, the CO_2 pressure was decompressed through a decompression-valve (controlled to be slightly lower than the K-point pressure), and the SCF-IL phases equilibrium shifts back to the VLLE equilibrium. In this situation, the overwhelming majority of the organic (product) had been extracted into the upper liquid and vapour CO_2 phases (Step IV, Scheme 3), and the resulting V + L1 phases (step IV, Scheme 3), which contained no detectable IL, were vented entirely into a solvent trap vessel with cooling apparatus by simple further decompression of the CO_2. The Ullmann products, biaryls, were collected through the valve on the bottom of the solvent trap vessel conveniently.

There are strong multiple forces, *e.g.* π–π stacking, hydrogen bonds, *etc.*, between hundreds of IL molecules and GO nanosheets. Previous reports revealed that the IL environment helps to stabilize the NP catalysts, therefore, the GO supported Pd NPs were inclined to remain in the bottom IL phase instead being extracted by the CO_2 phase. Further decompression of CO_2 led to easy isolation of the product without cross contamination of IL or catalyst. Once the product was isolated completely, fresh addition of reductant and substrate into the remained catalyst IL solution led to a new cycle of the Ullmann reaction (step I, Scheme 3).

The role of the CO_2 in the Ullmann reaction

A variety of reactions have been performed in the IL–$ScCO_2$ system. Most of such reports concerned the application of CO_2 as reaction media or reactants. The effect of CO_2 on catalyzed reactions in IL is not consistent throughout the literature sources. Some showed that CO_2 can increase the activity, while others indicate a decrease in activity with CO_2 pressure. Regardless, most studies consistently revealed an increase in selectivity (chemo-, regio-, and enantioselectivity). For example Tumas and co-workers[33] compared the results in a biphasic IL–CO_2 and IL–hexane system in olefin hydrogenation and found little difference in the reaction rate with pressurized CO_2 or hexane. Jessop and co-workers[34] performed asymmetric Ru-catalyzed hydrogenations in an IL–CO_2 biphasic system with enantioselectivity that was tunable with the pressure of CO_2. Leitner and co-workers[35] found that for iridium catalyzed hydrogenation of aromatic imines, an increase in reaction rate with the presence of CO_2 compared with H_2 pressure alone. There are also some recent studies that reveal that CO_2 acts as a substrate activating agent to promote the Ullmann reaction.[17f,36]

To identify the real role of the CO_2 in this reaction, a series of experiments on the Ullmann reaction of phenyl chlorides in the IL–$ScCO_2$ system were conducted. Experiments showed that CO_2 plays crucial role in the Ullmann reaction of aryl chlorides. In the absence of CO_2, no Ullmann coupling product was detected (entry 3, Table 1). When the CO_2 pressure was increased to 1 MPa, 4 MPa or 5.0 MPa (all were lower than the LCEP value, respectively), we still did not observe Ullmann coupling products (entries 6–8, Table 1). Further efforts found that when the pressure was increased to 6 MPa, a 27% yield of biphenyl was obtained (entry 9, Table 1). Interestingly, once the CO_2 pressure was higher than the LCEP pressure, an enhanced yield of Ullmann product was obtained (7.5 MPa, 60.0% yield, entry 10, Table 1). Encouraged by this, a series of experiments conducted at different CO_2 pressures was carried out. We found that an optimal yield of biphenyl was achieved when the pressure was controlled at 15.5 MPa (99.0% yield, entry 1, Table 1). Previous work had revealed that the [hmim][Tf_2N]/$ScCO_2$/n-nonanal system at 70 °C had a K-point of 13.61 MPa.[31a] In these experiments, we carried out the Ullmann reaction in [hmim][Tf_2N]–$ScCO_2$ at 45 °C. Experiments showed that once the pressure was increased over 12.90 MPa, which might be the K-point pressure for this system, a further increased yield would be obtained. For example, when the CO_2 pressure was controlled at 12.8 MPa (entry 11) a 69% yield was obtained, while when the pressure was increased to 13.0 MPa, a much enhanced yield was obtained (91%, entry 12, Table 1), indicating that K-point pressure plays important role in this reaction. Under such conditions, the SCF phase and the IL phase become critical and miscible to each other (near homogeneous manner[32]), therefore, the reaction can be carried out with much high activities.

In conclusion, CO_2 pressure plays important role in influencing the activity and conversion of the reaction. Apart from the role as an economical, environmentally friendly reaction media, CO_2also shows an apparent reaction activation effect on this reaction.

The catalyst and reducing agent

The aromaticity of the imidazolium cations and graphite layers (Fig. S2, ESI†) make them possess the possibility of π–π stacking, meanwhile, the structure of [hmim][Tf_2N] possesses nitrogen and hydrogen atoms in the imidazolium cation, serving as a weak H-bond donor.[37] Therefore there are strong multiple forces: π–π stacking, hydrogen bonds and electrosteric force between hundreds of [hmim][Tf_2N] molecules and exfoliated GO nanosheets. The bulkiness of IL imidazolium cations, N-imidazolium side chains together with anion of the IL favoured the electrosteric stabilisation of NPs, thus in this system, the IL phase was employed to sequester the catalyst and the CO_2 phase becomes the mobile phase for reactants and products. Why does Pd NP–GO have such high catalytic performance for the Ullmann reaction? We proposed that first the exfoliated GO nanosheets provided a relatively large surface area and high immobilization capacity on which to deposit highly active catalytic Pd NPs, which is very helpful for catalytic efficiency. Second, the Pd(0) NPs generated *in situ* by mild reduction can form smaller spherical Pd NPs (a median size distribution of 2–10 nm) dispersed uniformly over the few-layered exfoliated GO support, which exhibits superior catalytic performance.

As for the reducing agent, in the past decades, reagents such as aldehydes, hydrogen gas, carbon monoxide, ascorbic acid, amines, zinc, indium or germanium, *etc.* were used in the Ullmann reaction. Most of which are volatile or toxic, some of which are very expensive. In this work, we choose aluminium, which was much cheaper and readily available, as the reducing agent. In the presence of aluminium, the reductive Ullmann reaction of different aryl halides proceeded smoothly with a desired yield (entries 1, 21–28, Table 1), while when the reactions were carried out without addition of aluminium, only trace

Table 1 Pd NP catalyzed Ullmann reaction of aryl halides in IL–$ScCO_2$[a]

Entry	Aryl halide	CO_2[b] (MPa)	Prod.	Conv[c](%)	Yield[d](%)
1	chlorobenzene (**1a**)	15.5	**2a**	100	99
2[e]	chlorobenzene (**1a**)	15.5	**2a**	23	trace
3[f]	chlorobenzene (**1a**)	0	**2a**	31	n.d.[g]
4[h]	chlorobenzene (**1a**)	15.5	**2a**	59	42
5[i]	chlorobenzene (**1a**)	15.5	**2a**	83	56
6	chlorobenzene (**1a**)	1.0	**2a**	12	n. d.
7	chlorobenzene (**1a**)	4.0	**2a**	28	n. d.
8	chlorobenzene (**1a**)	5.0	**2a**	31	n. d.
9	chlorobenzene (**1a**)	6.0	**2a**	34	27
10	chlorobenzene (**1a**)	7.5	**2a**	72	60
11	chlorobenzene (**1a**)	12.8	**2a**	80	69
12	chlorobenzene (**1a**)	13.0	**2a**	97	91
13	bromobenzene (**1i**)	6.0	**2a**	42	33
14	iodobenzene (**1j**)	6.0	**2a**	62	55
15[j]	chlorobenzene (**1a**)	15.5	**2a**	13	n. d.
16[k]	chlorobenzene (**1a**)	15.5	**2a**	18	trace
17[l]	chlorobenzene (**1a**)	15.5	**2a**	15	trace
18[m]	chlorobenzene (**1a**)	15.5	**2a**	96	93
19[n]	chlorobenzene (**1a**)	15.5	**2a**	95	90
20[o]	chlorobenzene (**1a**)	15.5	**2a**	92	85
21	chloronaphthalene(**1b**)	15.5	**2b**	100	99
22[p]	1-*tert*-butyl-4-chlorobenzene (**1c**)	15.5	**2c**	100	99
23[q]	1-acetyl-4-chloro-benzene (**1d**)	15.5	**2d**	100	97
24[r]	2-chlorobenzyl alcohol (**1e**)	15.5	**2e**	99	96
25[s]	(2-chloro-vinyl)-benzene (**1f**)	15.5	**2f**	98	88
26[t]	1, 1-diphenyl-2-chloroethylene (**1g**)	15.5	**2g**	100	97
27[q]	4-chloroaniline (**1h**)	15.5	**2h**	98	95
28	4-chloro-2, 6-di-methyl-aniline (**1i**)	15.5	**2i**	99	93

[a] The reaction conditions were as follows: aryl halide (2 mM), Al (0) (108 mg), [hmim][Tf_2N] (3 ml); Pd NPs/GO (3.0% *w*/*w*, 186.2 mg) and $ScCO_2$ (15.5 MPa) at 45 °C for 10 h. [b] Pressure of CO_2. [c] Determined by GC analysis. [d] Isolated yield. [e] In the absence of Al (0). [f] In the absence of $ScCO_2$. [g] n. d. = no Ullmann products were detected. [h] In the absence of IL; some unidentified brown oil was also isolated. [i] Pd NP–GO (186.2 mg) in H_2O (3 ml) were used instead of Pd NP–GO in [hmim][Tf_2N]. [j] In the absence of GO. [k] Pd/C was used instead of Pd NPs/GO, the diameter of the Pd particles in which was 28–34 μm. [l] Pd NP–graphene (186.2 mg) was used instead of Pd NP–GO. [m] [bmim] [Tf_2N] was used instead of [hmim][Tf_2N]. [n] [hmim][BF_4] was used instead of [hmim][Tf_2N]. [o] [emim][Tf_2N] was used instead of [hmim][Tf_2N]. [p] The reaction time was 8 h instead of 10 h. [q] The reaction was conducted at 65 °C for 16 h. [r] Pd NP–GO (4% *w*/*w*, 248.3 mg) and 12 h were needed, some unidentified oil was also obtained. [s] Pd NP–GO (3.5% *w*/*w*, 217.3 mg) and 12 h were needed, some unidentified oil was also observed (2.47%). [t] Pd NP–GO (3.5% *w*/*w*, 217.3 mg) and 12 h were needed.

amounts of biaryl product were detected (entry 2, Table 1), indicating the crucial importance of aluminium as the reducing agent.

Reactions of different aryl halides

Though aryl bromide and aryl iodide are more active (the results in entries 9, 13 and 14 indicated their activity difference, Table 1), they are much more expensive than aryl chloride. Based on economical consideration, we choose the much cheaper aryl chloride, though less active, as the substrate. After a series of attempts, we found that in the presence of Al(0), the Pd NP–GO catalyzed reaction proceeded with 27% yield in [hmim][Tf_2N]/$ScCO_2$ system at 6 MPa (CO_2 pressure, entry 9, Table 1). Though the yield was still very low, it ignited our hope for further research indeed.

Encouraged by this, we tried further efforts. After a series of attempts, we found that when the pressure was increased to 15.5 MPa, the optimal yield of the Ullmann reaction of phenyl chloride was obtained (99%, entry 1, Table 1). Detail investigations showed that the optimal conditions for the Ullmann reaction were: biphenyl chloride (2 mM), Al (0) (108 mg), [hmim][Tf_2N] (3 ml); Pd NP–GO (3.0% *w*/*w*, 186.2 mg) and $ScCO_2$ (15.5 MPa) at 45 °C for 10 h (Scheme 4).

To study the efficiency and scope of the palladium nanoparticle-catalyzed Ullmann reaction of aryl chloride, the optimal reaction conditions were applied to a variety of aryl chlorides and the results are summarized in Table 1 (entries 1 and 21–28, Table 1). As shown in Table 1, the Ullmann reaction of various aryl chlorides (**1a–1i**), bearing different substituents runs smoothly in the IL–$ScCO_2$ system in the presence of Al(0) and Pd NP–GO. The results in Table 1 also indicate that the reaction rate depends on the structure of the aromatic chloride. For instance, aryl chloride **1c**, which bears an electron-donating substituent, needs a shorter reaction period (8 h, entry 22, Table 1) compared with aryl chlorides **1a** and **1b** (10 h, entries 1, 21, Table 1). When aryl chlorides bearing electron-withdrawing substituents were studied (e. g. **1d**), a longer reaction time and higher reaction temperature were needed, for example, for the reaction of **1d**, the substrate was converted into **2d** readily in a 97% yield after 16 h (entry 23, Table 1). For aryl chloride **1h**,

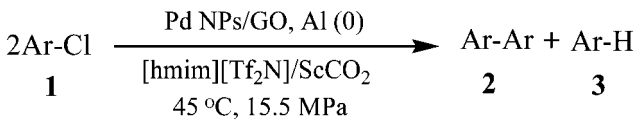

Scheme 4 Pd NPs catalyzed reductive Ullmann reaction of aryl chloride.

which also contained an electron-withdrawing substituent ($-NH_2$) in its structure, the Pd NP-catalyzed Ullmann reaction of **1h** can proceed smoothly with desired yields (95%, entry 27, Table 1) with reaction times of 16 h. While for aryl chloride **1i**, which bears both electron-pushing and electron-withdrawing substituents in the structure, the reaction run smoothly with a 93% yield of **2i** (entry 28, Table 1) without prolonging the reaction time, indicating the overlapping effect of these two types of substituents. Meanwhile, we also noticed that aryl chlorides with ene structures, **1f–g**, had long reaction times compared with **1a** and **1b**, and homocoupling products **2f–2g** were afforded in good yields (88% and 97%, respectively, entries 25–26 Table 1).

Catalyst support and active hydrogen donor

In conventional work,[17f] H_2O or alcohol was selected as a precursor of hydrogen, providing abundant active hydrogen. However, the use of H_2O led to difficult product separation and complicated phase behaviour in the reaction system. For example, when IL was replaced by H_2O, the PdNP–GO catalyzed Ullmann reaction proceeded with an 83% conversion, while the isolated yield was only 56% (entry 5, Table 1), indicating a decreased isolation efficiency of the Ullmann product. This can be explained by inferior inter-miscible behaviour of H_2O and $ScCO_2$ in the H_2O–$ScCO_2$ system. In fact, we anticipated that we can use an active hydrogen donor without loss of the product isolation efficiency. Therefore, trying to find an alternative active hydrogen donor matching such requirements is necessary. This is a big challenge indeed.

Bearing large amounts of carboxylic, hydroxyl, aldehyde groups in the structure, GO nanosheets were anticipated to release active hydrogen atoms. Significantly, after a series of efforts, we found that GO can replace the traditional active hydrogen donor readily, and investigations showed that when catalyzed by PdNP–GO, the Ullmann reaction of various aryl chlorides was carried out well with good yields (**1a–i**, entries 1, 21–28, Table 1). In the absence of H_2O, such results indicated that GO can replace the traditional active hydrogen donors. Further investigations also proved the important role of GO as an active hydrogen donor. Experimental results showed that in the absence of GO, no biaryl product was observed (entry 15, Table 1), and when Pd/C, which did not contain any active hydrogen, was used instead of Pd NP–GO, only trace amounts of Ullmann products were detected (entry 16, Table 1). Similarly, when Pd NPs (synthesized by the same method as described in experimental section, except that there was no GO involved) were chosen to replace the catalyst Pd NP–GO, a trace signal of biaryl product was observed (entry 17, Table 1), revealing that GO was important in providing active hydrogen to finish the reductive Ullmann cycle.

Product separation

In the IL–$ScCO_2$ system, CO_2 extraction provides an efficient method for product isolation. In our experiments, by simple depressurization of CO_2, the biaryl products, which finally exhibited a solvent-free and analytically pure form as a colourless crystalline material, can be isolated easily from the catalyst solution of IL by CO_2 extraction without cross contamination of IL or catalyst. In the experiments summarized in Table 1, no signals associated with the IL were detected during NMR and GC-MS analyses of the products. Samples from each run were analyzed by ICP measurement, demonstrating that the palladium content was below the detection limit of the instrument (<1 ppm) in all cases, and that no significant leaching of metal compounds into the products had occurred. All above results showed that the environmentally friendly IL–$ScCO_2$ system can provided high efficient product separation route for Ullmann product.

IL and catalyst recycling

Although most ILs have no measurable vapour pressure, and, thus, no air pollution potential, they are considered as "green" media, however, toxicity in soil and water eco-systems must be carefully understood. The optimal method would be to recycle the IL in these reactions. For economic consideration, most IL are quite expensive and IL recycling would be the best choice. Meanwhile, the Pd NPs show a relatively strong trend toward agglomeration. In most catalytic reactions, it's necessary to use an additional stabiliser or a solid support material.

Here, Pd NPs support of exfoliated GO with wrinkles was one of the ways to prevent Pd NPs from agglomeration. In addition, the IL environment can also help to stabilize the NP catalysts, and the IL solutions of catalyst were significantly less air sensitive than catalyst solutions in conventional organic solvents. It is assumed that the bulkiness of the IL imidazolium cations favour the electrosteric stabilisation of NPs, and the N-imidazolium side chains as well as the anions of the IL can also stabilise the metal (0) NPs due to electronic interaction with the metal surface.[4,37]

In our experiments, we found that excellent catalytic activities can be achieved for at least 5 runs. The conversions for the first, second, third and forth runs were 100%, 99%, 99% and 100%, respectively (entries 1–4, Table 2), and slightly declined conversion for the fifth and sixth runs (98% and 95%, respectively, entries 5, 6, Table 2).

In the first cycle, the numbers of –OH and –COOH groups are much larger than the numbers of Pd surface sites, thus the reaction runs readily with good performance. However, for further cycles, if no fresh GO was added to the reaction system, the conversion for the second run of the reaction drops to 95%, and then drops to 81% for the third run, 57% and 24% for the cycles thereafter. After ten runs, the conversion became very low (entries 1–6, Table 2), because as a novel active hydrogen donor, each catalytic cycle would consume a large amount of –OH and –COOH groups on GO. Therefore, before each subsequent run, GO (40 mg) should be added to the catalyst–IL solution in the stainless vessel to ensure the numbers of –OH and –COOH groups are much larger than the numbers of Pd surface sites for good cycle performance.

Investigations also revealed that the recycling performance of the catalyst in IL–$ScCO_2$ showed superior advantages over other reaction media combined with $ScCO_2$. For example, when the H_2O–$ScCO_2$ system was chosen to replace IL–$ScCO_2$, the conversion for the first and second runs were 78% and 53%, respectively (entries 1–2, Table 2), and sharply declined conversion for the third and forth run (39% and 17%, respectively,

Table 2 The Ullmann reaction of phenyl chloride in [hmim][Tf_2N]–$ScCO_2$ (conversion as a function of the number of the cycles)[a]

Entry	Catalyst solution[b]	Conversion (%)[c] for [hmim][Tf_2N]–$ScCO_2$	Conversion (%) for H_2O–$ScCO_2$
1	Fresh	100	78
2	Recycled from run 1	99 (95)	53
3	Recycled from run 2	99 (81)	39
4	Recycled from run 3	100 (57)	17
5	Recycled from run 4	98 (24)	—
6	Recycled from run 5	95 (18)	—

[a] Formation of biphenyl. [b] Before each subsequent run, phenyl chloride (2 mM), GO (40 mg) and Al (0) (108 mg) were added to the catalyst–[hmim][Tf_2N] or H_2O solution in the stainless vessel. [c] The numbers in the brackets were the conversions without addition of GO.

entries 3–4, Table 2). All sharply decreased compared with the conversions obtained in the corresponding cycle in IL–$ScCO_2$, indicating the inferior efficiency of the H_2O–$ScCO_2$ system. In fact, the IL plays an important role in the recycling of the Pd NP–GO catalyst. As stated above, the IL environment helps to stabilize the NP catalysts. This is observed in TEM and SEM images shown in Fig. S1 (ESI†). As shown in Fig. S1a, b (ESI†), when IL was used in the recycling cycles, no obvious Pd NP catalyst agglomeration was found after 3 cycles. The diameters of the Pd NPs were still in small scales and a narrow range similar to the diameters for the first run (Fig. 1a, 1d). While when the IL was alternated by H_2O, serious Pd NP agglomeration occurred after 3 runs of the reaction (Fig. S1c,d, ESI†). Such results can explain the sharp declination of conversion in the recycling experiments of the H_2O–$ScCO_2$ system, indicating that the IL was a high efficient stabiliser for Pd NPs.

Possible mechanism for the Ullmann reaction

Based on previous work,[14,15,38] a plausible mechanism for the Pd NP–GO catalyzed reductive Ullmann reaction of aryl chloride is shown in Scheme 5. In this process, carbon dioxide can react with GO at high pressure generating carbonic acid (H_2CO_3), which then produces H_2 by reacting with Al(0). To begin with, a single electron transfer (SET) process could occur from a Pd (0) supported on GO to an ArCl molecule, forming a $[ArX]^-$ radical anion and a positively charged Pd^+ to give intermediate **5**. Dissociation of $[ArX]^-$ would give Ar˙ and X^-, forming intermediate **6**, then the intermediate **6** reacts with another **1a** molecule giving intermediate **7**, successively, coupling two aryl radicals would give the biaryl product **2** and $PdCl_2$. The obtained $PdCl_2$ can be reduced by H_2 to regenerate the active Pd(0) species readily to finish the cycle. It is noteworthy that a primary side-reaction would occur at the same time. Firstly, Pd(0) could also react with H_2 giving intermediate **9** ($Pd^{2+}(H^-)_2$), which could then react with **1a** affording the main side product Ar–H (**3**). Thus the greatest challenge might be how to minimize the possibility of the side reaction forming side-product **3**. Fortunately, in this reaction, in the presence of $ScCO_2$ at high pressure, no obvious side-products have been detected. It is assumed that CO_2 could insert into the Pd–H bond of **9** taking place to form Pd $(OOCH)_2$ (**10**). With CO_2 insertion, much more enhanced steric hindrance was achieved in intermediate **10** than intermediate **9**, the barricaded intermediate **10** was inclined to react with HCl readily affording the active Pd (0) species instead of reaction with **1a** giving side-product **3**. Therefore, in the presence of $ScCO_2$, the reaction proceeded with high selectivity towards the Ullmann coupling product **2**. Such SET mechanism was also confirmed by MALDI-TOF MS analysis.[39] As we can see from Fig. S3a (ESI†), Pd NP–GO (**4**) holds typical mass peaks at 16, 17, 29 and 44, which belong to epoxy, hydroxyl, aldehyde and carboxyl groups on GO, respectively. As the number of cycles increases, the mass peaks for GO become weaker (Fig. S3b and Fig. S3c, ESI†), which indicates that the reaction would consume large amounts of –OH and –COOH groups on GO. Moreover, Fig. S3b shows strong peaks at 77.1, 112.1 and 114.1, which are typical mass peaks for ArCl This suggests that it is possible to form intermediate **5** as shown Scheme 5. Similarly, by MALDI-TOF MS analysis, we detect strong peaks for the biphenyl product (153.0 and 76.0 *etc.*), showing the successful Ullmann reaction in the IL–$ScCO_2$ system catalyzed by Pd NP–GO.

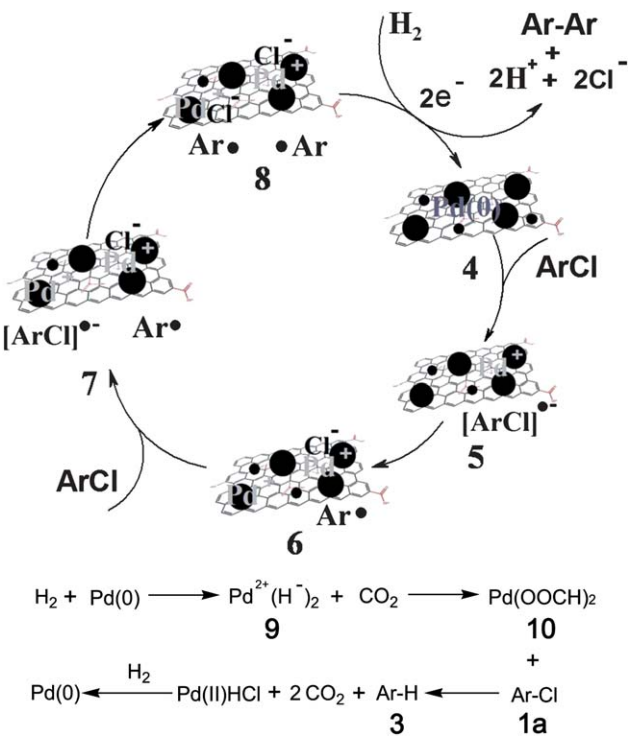

Scheme 5 Possible mechanism for the Pd NP–GO catalyzed Ullmann reaction of aryl chloride.

Conclusions

In conclusion, we have demonstrated an environmentally friendly process: high active and recyclable graphene oxide-supported palladium nanoparticle-catalyzed reductive Ullmann reaction of aryl chlorides in ionic liquid–supercritical carbon dioxide system. The application of cheaper chemicals, such as aryl chlorides (instead of expensive aryl bromides or iodides), aluminium (instead of expensive zinc or indium, *etc.*) and naturally abundant "greenhouse" gas CO_2, make this kind of process quite attractive. The Pd NP catalyst and ionic liquid can be recycled for at least 5 runs, indicating the economic viability of this process. The employment of the ionic liquid–supercritical carbon dioxide system led to immobilization, activation, and stabilization of the Pd NP catalyst that would be impossible in classical organic media separately. GO, the novel catalyst support, was found to replace the traditional active hydrogen donor readily with much enhanced product separation efficiency. Carbon dioxide, a naturally abundant, nonflammable, relatively nontoxic, economical and recyclable "greenhouse" gas, was found to significantly promote the selectivity of the Pd NP-catalyzed aluminium-induced reductive Ullmann reaction of aryl chlorides. Further studies on the phase behaviours of different ionic liquids in supercritical carbon dioxide for different coupling reaction are under progress in our laboratory.

Acknowledgements

We are grateful to the Scientific Foundation of Guangxi Zhuang Autonomous Region of China (No. 200626152, 200508193, 200925066) for financial support.

References

1 (*a*) W. Leitner, *Nature*, 2003, **423**, 930–931; (*b*) M. Benaglia. *Recoverable and Recyclable Catalysts*. John Wiley&Sons, Ltd.: Chichester. 2009; (*c*) F. M. Kerton. *Alternative Solvents for Green Chemistry*. Royal Society of Chemistry. Cambridge. 2009; (*d*) I. Ojima. *Catalytic Asymmetric Synthesis*, 2nd ed. VCH: Weinheim, 2000; (*e*) R. Noyori, *Acc. Chem. Res.*, 1990, **23**, 345–350.
2 (*a*) S. V. Dzyuba and R. A. Bartsch, *Angew. Chem., Int. Ed.*, 2003, **42**, 148–150; (*b*) U. Hintermair, T. Höfener, T. Pullmann, G. Franciò and W. Leitner, *ChemCatChem*, 2010, **2**, 150–154; (*c*) L. A. Blanchard, D. Hancu, E. J. Beckman and J. F. Brennecke, *Nature*, 1999, **399**, 28–29; (*d*) S. N. V. K. Aki, B. R. Mellein, E. M. Saurer and J. F. Brennecke, *J. Phys. Chem. B*, 2004, **108**, 20355–20365.
3 (*a*) R. A. Brown, P. Pollet, E. McKoon, C. A. Eckert, C. L. Liotta and P. G. Jessop, *J. Am. Chem. Soc.*, 2001, **123**, 1254–1255; (*b*) M. Harada, C. Kawasaki, K. Saijo, M. Demizu and Y. Kimura, *J. Colloid Interface Sci.*, 2010, **343**, 537–545.
4 F. Jutz, J. Andanson and A. Baiker, *J. Catal.*, 2009, **268**, 356–366.
5 P. B. Webb, M. F. Sellin, T. E. Kunene, S. Williamson, A. M. Z. Slawin and D. J. Cole–Hamilton, *J. Am. Chem. Soc.*, 2003, **125**, 15577–15588.
6 B. Yoon, C. H. Yen, S. Mekki, S. Wherland and C. M. Wai, *Ind. Eng. Chem. Res.*, 2006, **45**, 4433–4435.
7 (*a*) D. W. Goodman, *Nature*, 2008, **454**, 948–949; (*b*) J. Han, Y. Liu and R. Guo, *J. Am. Chem. Soc.*, 2009, **131**, 2060–2061; (*c*) V. Cimpeanu, M. Kočevar, V. I. Parvulescu and W. Leitner, *Angew. Chem. Int. Ed.*, 2009, **121**, 1105–1108; (*d*) T. N. Glasnov, S. Findenig and C. O. Kappe, *Chem.–Eur. J.*, 2009, **15**, 1001–1010; (*e*) L. X. Yin and J. Liebscher, *Chem. Rev.*, 2007, **107**, 133–173; (*f*) D. Astruc, F. Lu and J. R. Aranzaes, *Angew. Chem., Int. Ed.*, 2005, **44**, 7852–872; (*g*) G. Ertl, H. Knözinger, F. Schüth, J. Weitkamp. *Handbook of Heterogeneous Catalysis*, 2nd ed., Wiley–VCH, Weinheim, 2008.
8 (*a*) A. K. Geim, *Science*, 2009, **324**, 1530; (*b*) S. J. Park and R. S. Ruoff, *Nat. Nanotechnol.*, 2009, **4**, 217; (*c*) A. K. Geim and K. S. Novoselov, *Nat. Mater.*, 2007, **6**, 183; (*d*) J. L. Xia, F. Chen, J. H. Li and N. J. Tao, *Nat. Nanotechnol.*, 2009, **4**, 505; (*e*) L. H. Tang, Y. Wang, Y. M. Li, H. B. Feng, J. Lu and J. H. Li, *Adv. Funct. Mater.*, 2009, **19**, 2782; (*f*) X. L. Dong, J. S. Cheng, J. H. Li and Y. S. Wang, *Anal. Chem.*, 2010, **82**, 6208–6214; (*g*) H. X. Chang, L. H. Tang, Y. Wang, J. H. Jiang and J. H. Li, *Anal. Chem.*, 2010, **82**, 2341–2346; (*h*) L. H. Tang, H. B. Feng, J. S. Cheng and J. H. Li, *Chem. Commun.*, 2010, **46**, 5882–5884; (*i*) Q. Zeng, J. S. Cheng, J. H. Li and J. H. Jiang, *Adv. Funct. Mater.*, 2010, **20**, 3366–3372.
9 (*a*) Y. M. Li, L. H. Tang and J. H. Li, *Electrochem. Commun.*, 2009, **11**, 846–849; (*b*) G. M. Scheuermann, L. Rumi, P. Steurer, W. Bannwarth and R. Mülhaupt, *J. Am. Chem. Soc.*, 2009, **131**, 8262–8270; (*c*) C. Xu, X. Wang and J. W. Zhu, *J. Phys. Chem. C*, 2008, **112**, 19841–19845; (*d*) H. Zhang, X. J. Lv, Y. M. Li, L. M. Li and J. H. Li, *ACS Nano*, 2010, **4**, 380–386; (*e*) H. X. Chang, H. Zhang, X. J. Lv and J. H. Li, *Electrochem. Commun.*, 2010, **12**, 483–487.
10 (*a*) D. R. Dreyer, H.-P. Jia and C. W. Bielawski, *Angew. Chem.*, 2010, **122**, DOI: 10.1002/ange.201002160; (*b*) W. W. Cai, R. D. Piner, F. J. Stadermann, S. Park, M. A. Shaibat, Y. Ishii, D. X. Yang, A. Velamakanni, S. J. An, M. Stoller, J. H. An, D. M. Chen and R. S. Ruoff, *Science*, 2008, **321**, 1815–1817; (*c*) D. A. Dikin, S. Stankovich, E. J. Zimney, R. D. Piner, G. H. B. Dommett, G. Evmenenko, S. T. Nguyen and R. S. Ruoff, *Nature*, 2007, **448**, 457–460; (*d*) Y. Wang, Z. H. Li, D. H. Hu, C.-T. Lin, J. H. Li and Y. H. Lin, *J. Am. Chem. Soc.*, 2010, **132**, 9274–9276; (*e*) T.-F. Yeh, J.-M. Syu, C. Cheng, T.-H. Chang and H. Teng, *Adv. Funct. Mater.*, 2010, **20**, 2255–2262; (*f*) J. H. Jung, D. S. Cheon, F. Liu, K. B. Lee and T. S. Seo, *Angew. Chem., Int. Ed.*, 2010, **49**, DOI: 10.1002/anie.201001428.
11 (*a*) L. J. Gooßen, G. J. Deng and L. M. Levy, *Science*, 2006, **313**, 662–664; (*b*) R. H. Thomson, *The Chemistry of Natural Products*, Blackie and Son, Glasgow, 1985; (*c*) O. Baudoin, M. Cesario, D. Guenard and F. Guéritte, *J. Org. Chem.*, 2002, **67**, 1199–1207.
12 K. C. Nicolaou, C. N. C. Boddy, S. Bräse and N. Winssinger, *Angew. Chem., Int. Ed.*, 1999, **38**, 2096–2152.
13 (*a*) I. Capanec. *Synthesis of Biaryls*, Elsevier, Oxford, 2004; (*b*) *Supramolecular Chemistry*, 1st ed. (Ed.: J. M. Lehn), VCH, Weinheim, 1995.
14 X. F. Mei and W. C. Christian, *J. Am. Chem. Soc.*, 2006, **128**, 13326–13327.
15 J. Roncali, *Chem. Rev.*, 1992, **92**, 711–738.
16 (*a*) L. Fogel, R. P. Hsung, W. D. Wulff, R. D. Sommer and A. L. Rheingold, *J. Am. Chem. Soc.*, 2001, **123**, 5580–5581; (*b*) A. V. Vorogushin, W. D. Wulff and H.-J. Hansen, *J. Am. Chem. Soc.*, 2002, **124**, 6512–6513.
17 (*a*) F. Ullmann and J. Bielecki, *Ber. Dtsch. Chem. Ges.*, 1901, **34**, 2174–2185; (*b*) F. Ullmann, G. M. Meyer, O. Loewenthal and E. Gilli, *Justus Liebigs Ann. Chem.*, 1904, **332**, 38–81; (*c*) Y. Wang, H. Y. Wang, F. Q. Zhao, K. Klingstedt, O. Terasaki and D. Y. Zhang, *J. Am. Chem. Soc.*, 2009, **131**, 4541–4550; (*d*) H. Y. Wang and Y. Wan, *J. Mater. Sci.*, 2009, **44**, 6553–6562; (*e*) V. Calò, A. Nacci, A. Monopoli and P. Cotugno, *Chem.–Eur. J.*, 2009, **15**, 1272–1279; (*f*) J. H. Li, Y. X. Xie and D. L. Yin, *J. Org. Chem.*, 2003, **68**, 9867–9869; (*g*) J. Z. Jiang and C. Cai, *Colloids Surf., A*, 2007, **305**, 145–148.
18 For recent reviews, see:(*a*) T. D. Nelson and R. D. Crouch, *Org. React. (N.Y.)*, 2004, **63**, 265–555; (*b*) F. Monnier and M. Taillefer, *Angew. Chem., Int. Ed.*, 2008, **47**, 3096–3099; (*c*) F. Monnier and M. Taillefer, *Angew. Chem., Int. Ed.*, 2009, **48**, 6954–6971.
19 (*a*) R. A. Altman and S. L. Buchwald, *Nat. Protoc.*, 2007, **10**, 2474–2479; (*b*) J. T. Zhang, Z. H. Zhang, Y. Wang, X. Q. Zheng and Z. Y. Wang, *Eur. J. Org. Chem.*, 2008, 5112–5116.
20 S. Mukhopadhyay, G. Rothenberg, H. Wiener and Y. Sasson, *Tetrahedron*, 1999, **55**, 14763–14768.
21 D. L. Boger, J. Goldberg and C.-M. Andersson, *J. Org. Chem.*, 1999, **64**, 2422–2427.
22 H. Amii, M. Kohda, M. Seo and K. Uneyama, *Chem. Commun.*, 2003, 1752–1753.
23 R. N. Ram and V. Singh, *Tetrahedron Lett.*, 2006, **47**, 7625–7628.
24 M. Kuroboshi, Y. Waki and H. Tanaka, *J. Org. Chem.*, 2003, **68**, 3938–3942.

25 L. Wang, Y. H. Zhang, L. F. Liu and Y. G. Wang, *J. Org. Chem.*, 2006, **71**, 1284–1287.
26 N. Shezad, A. A. Clifford and C. M. Rayner, *Green Chem.*, 2002, **4**, 64–67.
27 J. H. Li, Y. X. Xie, H. F. Jiang and M. C. Chen, *Green Chem.*, 2002, **4**, 424–425.
28 W. S. Hummers and R. E. Offeman, *J. Am. Chem. Soc.*, 1958, **80**, 1339.
29 X. Li, X. Wang, L. Zhang, S. Lee and H. J. Dai, *Science*, 2008, **319**, 1229.
30 (*a*) Y. Wang, Y. M. Li, L. H. Tang, J. Lu and J. H. Li, *Electrochem. Commun.*, 2009, **11**, 889–892; (*b*) Y. X. Xu, H. Bai, G. W. Lu, C. Li and G. Q. Shi, *J. Am. Chem. Soc.*, 2008, **130**, 5856–5857.
31 (*a*) A. Ahosseini, W. Ren and A. M. Scurto, *Ind. Eng. Chem. Res.*, 2009, **48**, 4254–4265; (*b*) J.-M. Andanson and F. Jutz, *J. Phys. Chem. B*, 2009, **113**, 10249–10254; (*c*) J.-Y. Ahn, B.-C. Lee, J. S. Lim, K.-P. Yoo and J. W. Kang, *Fluid Phase Equilib.*, 2010, **290**, 75–79.
32 M. C. Kroon, L. J. Florusse, L. J. Kühne, G. I. Witkamp and C. J. Peter, *Ind. Eng. Chem. Res.*, 2010, **4**, 3474–3478.
33 F. Liu, M. B. Abrams, R. T. Baker and W. Tumas, *Chem. Commun.*, 2001, 433–434.
34 R. A. Brown, P. Pollet, E. McKoon, C. A. Eckert, C. L. Liotta and P. G. Jessop, *J. Am. Chem. Soc.*, 2001, **123**, 1254–1255.
35 M. Solinas, A. Pfaltz, P. G. Cozzi and W. Leitner, *J. Am. Chem. Soc.*, 2004, **126**, 16142–16147.
36 H. X. Li, C. Wei and Z. Fang, *Chin. J. Chem.*, 2008, **26**, 25–29.
37 (*a*) H. Olivier–Bourbigou, L. Magna and D. Morvan, *Appl. Catal., A*, 2010, **373**, 1–56; (*b*) Y. Hu, H. Yang, Y. Zhang, Z. Hou, X. Wang, Y. Qiao, H. Li, B. Feng and Q. Huang, *Catal. Commun.*, 2009, **10**, 1903–1907; (*c*) D. Astruc, *Inorg. Chem.*, 2007, **46**, 1884–1894.
38 (*a*) J. S. Cheng and H. F. Jiang, *Eur. J. Org. Chem.*, 2004, 643–646; (*b*) J. S. Cheng, G. F. Wei, J. Zhao, S. W. Huang and Z. L. Huang, *Res. Chem. Intermed.*, 2006, **32**, 887–894; (*c*) L. D. Pachón, C. J. Elsevier and G. Rothenberg, *Adv. Synth. Catal.*, 2006, **348**, 1705–1710.
39 X. L. Dong, J. S. Cheng, J. H. Li and W. S. Wang, *Anal. Chem.*, 2010, **82**, 6208–6214.

